Chemical Process Design Vol.5 No.2 (2026) 135-148

University of Sistan and Baluchestan

Chemical Process Design

Available online at http://cpd.usb.ac.ir/

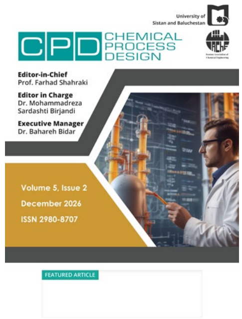

Continuous Biosorption of Co (II) onto Mg-Modified *Sargassum sp.* Brown Algae in a Fixed Bed Column

Mohammad Hassan Khani[1]✉, Ali Asghar Ghorbanpour Khamseh[2], Younes Amini[3]

[1] Corresponding Author, Nuclear Fuel Cycle Research School, Nuclear Science and Technology Research Institute, Tehran, Iran.
Email: mhkhani@aeoi.org.ir
[2] Nuclear Fuel Cycle Research School, Nuclear Science and Technology Research Institute, Tehran, Iran.
Email: akhamseh@aeoi.org.ir
[3] Nuclear Fuel Cycle Research School, Nuclear Science and Technology Research Institute, Tehran, Iran.
Email: yamini@aeoi.org.ir

ARTICLE INFO

Article type:
Research Article

Article history:
Received: 2026-06-28
Received in revised form: 2026-08-10
Accepted: 2026-08-18
Available online: 2026-08-18

Keywords: *Biosorption; Cobalt; Sargassum sp. brown algae; Mg-modification; Breakthrough curve; Fixed bed column*

ABSTRACT

In this research, the potential of *Sargassum sp.* brown algae was studied to adsorb cobalt from aqueous solutions in a fixed bed column. The effects of key operating parameters, including feed flow rate (1–4 mL/min), bed height (4–9 cm), and inlet cobalt concentration (50–150 mg/L), on uptake were investigated. FTIR analysis was performed to identify the vibrational variations associated with the surface functional group peaks. The FTIR tests showed that hydroxyl, amine, amide, methylene and carboxyl functional groups may have the greatest contribution in the ion exchange mechanism. Moreover, SEM analysis was conducted to investigate the morphological variations in the biosorbent due to the sorption process. Under the studied conditions, the maximum adsorption in the column was achieved at a flow rate of 1 mL/min, a bed height of 9 cm, and an initial influent concentration of 150 mg/L, reaching 79.83 mg/g. Adsorption breakthrough curves were modeled using Thomas, Yoon-Nelson and Adams–Bohart models. Among the evaluated breakthrough models, the Thomas model provided the most suitable description of Co(II) adsorption behavior, yielding a maximum adsorption capacity of q_{Th}=81.93 mg/g and a Thomas rate constant of k_{Th}=1.15×10−5 L/min.mg. These results suggest that *Sargassum sp.* can be considered a promising and efficient option for cobalt removal from aqueous solutions in water treatment processes.

Cite this article: Khani, M.H., Ghorbanpour Khamseh, A.A., Amini, Y., (2026), Continuous Biosorption of Co (II) onto Mg-Modified *Sargassum sp.* Brown Algae in a Fixed Bed Column, *Chemical Process Design*, 5(2), 135-148. http//doi.org/10.22111/cpd.2026.55990.1093

DOI: http//doi.org/10.22111/cpd.2026.55990.1093

Publisher: University of Sistan and Baluchestan.

1. Introduction

Heavy metal pollutants and radionuclides are one of the most important concerns for the environment because of their toxicity impacts on plants, animals and humans [1]. Cobalt-based compounds are extensively applied in various industrial sectors, including mining, metallurgical, electroplating, paints, petrochemical, electronic, and nuclear power plants [2]. Acute cobalt poisoning in humans can lead to severe health issues such as allergic reactions, vomiting, neurological disturbances, and damage to vital organs including the heart, thyroid, and liver. Prolonged exposure may also result in a reduced or complete loss of smell and various gastrointestinal disorders [3-6]. Therefore, removing cobalt from aqueous solutions is necessary and vital due to environmental issues and human health.

To recover and remove metal ions from aqueous solutions and wastewater, several treatment methods have been developed, including chemical precipitation [7,8], solvent extraction [9-12], ion exchange[13-15], membrane processes[16,17], and adsorption[18-22]. The performance, cost, and environmental impact of these methods depend strongly on the specific operating conditions and application context. Among them, adsorption has attracted considerable attention as an effective approach for addressing environmental pollution issues [23].

Biosorbents such as algae, yeast, fungi, and bacteria, are of interest to many researchers due to their advantages such as high efficiency, cheapness and availability in removing heavy metal ions from wastewater [24-27]. Algal biomass comprising microalgae, macroalgae, and cyanobacteria offers several advantages over other types of microbial biomass because of its diverse morphology, scalability, and the variety of valuable products that can be obtained through industrial and fermentation processes [28-32]. Several studies have documented cobalt removal by different algal species, including *Sargassum*, *Ulva*, *Dunaliella sp.*, *Padina pavonica* [18, 33-35]. Previous studies have reported that the brown alga *Sargassum sp.* efficiently adsorbs and removes a wide range of heavy metals and radionuclides, such as Co, U, Th, Sr, Cu, Zn, Cd, and Ni, from aqueous media. [30, 34, 36-38].

Given the promising results of cobalt adsorption by magnesium-modified *Sargassum sp.* brown algae in batch experiments reported in our previous work (34), this study aims to investigate cobalt biosorption process using magnesium-modified *Sargassum sp.* algae in a continuous system for the first time. From a practical point of view, large scale biosorption processes are continuous and are generally carried out in fixed bed columns. Fixed-bed systems are considered promising for practical applications; however, their scale-up requires careful consideration of hydrodynamics, pressure drop, mass transfer, regeneration, feed variability, and mechanical stability [39-41].

The fixed bed column and its performance are described using the breakthrough curve (concentration-time diagram). For this reason, in this research, empirical models were used to model breakthrough curve. Also, investigating the adsorption mechanism and determining the effective functional groups in the adsorption process of cobalt is one of the other goals of this research.

2. Material and methods

2.1. Reagents and solutions

To prepare cobalt solutions at various concentrations, a stock solution with a concentration of 1000 mg/L was first prepared using analytical-grade cobalt nitrate hexahydrate ($Co(NO_3)_2 \cdot 6H_2O$) dissolved in distilled water. Subsequently, the required test solutions were obtained by carefully diluting this stock solution. The pH of the solutions was adjusted using 1 M sodium hydroxide and 1 M nitric acid as needed. All chemicals and reagents used in this study were of analytical grade and purchased from Sigma-Aldrich, Germany.

2.2. Preparation of biosorbent

Heavy Samples of marine algae *Sargassum sp.* were collected from the coast of Qeshm, in the Persian Gulf, identified, and supplied by the Hormozgan Agricultural and Natural Resources Research and Education Center. The algal samples were then washed with tap water and distilled water to remove sand and excess of sodium and potassium ions. After drying overnight at a maximum temperature of 55 ºC to avoid degradation of the binding sites [10], the samples were grounded to an average particle size of 0.7 mm. The biomasses were subsequently loaded with Mg^{2+} in a solution of 0.1 M $Mg(NO_3)_2.6H_2O$ at pH 4 (biomass concentration of 10 g/l) for 24 h under slow stirring at 100 rpm and 25 ºC. Then pretreated biomass was washed several times with deionized water until a stable wash solution pH was reached and excess magnesium ions removed from the biomasses. The Mg-pretreated biomasses were then dried overnight in an oven at 55 ºC and subsequently Mg-pretreated algae used for biosorption experiments [30].

2.3. Characterization and analyses

An inductively coupled plasma atomic emission spectrometer, ICP-AES model 7300 DV USA, was used to analyze cobalt concentration in solutions. A pH-meter (744 Metrohm Herisau, Switzerland) was employed to evaluate the pH values of the solutions. A scanning electron microscopy, SEM Hitachi S-4160 Japan, was employed to analyze the morphology of the biosorbent. Fourier transform infrared spectroscopy (FTIR), Bruker Optik GmbH, model IFS 88 Germany, was used to characterize the biosorbent in the range of 400–4000 cm^{-1}.

2.4. Column sorption procedure

Cobalt (II) biosorption experiments were performed in an acrylic fixed bed column with a height of 20 cm and an internal diameter of 2.54 cm. Two holders including a metal grid with 0.5 mm holes connected to a plastic cylinder with an external diameter of 2.54 cm and a height of 1 cm were installed to keep the substrate stable at the bottom and top of the column. For the 4 cm bed height used in the experiments, the corresponding packed adsorbent mass was 3 g, with a bulk density of 0.148 g/cm^3. Using a particle density of 0.471 g/cm^3, the bed porosity was estimated to be 0.686. The algae were packed in the column, and the test solution was pumped upstream through the bed using a peristaltic pump (Watson Marlow Pump, model 205U) at a constant inlet velocity. All experiments were performed at room temperature. The pH of the test solution was adjusted to the optimal pH of 7 [34] using 0.1 M HNO_3 and 0.1 M NaOH solutions.

Experiments were carried out under different operating conditions, with varying flow rate, bed height and initial concentration of test solution. The effluent solution was collected from the top of the column at regular intervals and the residual concentration was measured using ICP-AES. Column operation was stopped when the effluent concentration exceeded 99.5% of its initial concentration. To minimize errors, all experiments were performed in duplicate.

2.5. Packed bed column sorption parameters

The breakthrough curve for a column is obtained by plotting C/C_0 (C and C_0 are the concentrations in the inlet and outlet, respectively) against time. The adsorption capacity of the column (adsorbed mass (mg) per unit of dry adsorbent mass (g)) during the operating interval of the column (t_{total}) can be calculated using the following equation [42]:

$$q = \frac{m_{ad}}{M} \tag{1}$$

where q is the adsorption capacity (mg/g), M is the dry mass of the adsorbent in the column (g), m_{ad} is the mass of the adsorbate adsorbed onto solid phase (mg) which is calculated by the following equation [42]:

$$m_{ad} = QC_0 \int_0^{t_{total}} \left(1 - \frac{C}{C_0}\right) dt \tag{2}$$

where Q (mL/min) is the flow rate of the inlet solution and t_{total} (min) is column operation time.

The percentage removal efficiency (R%) in the fixed bed column is calculated using the following equation [43]:

$$R\% = \frac{m_{ad}}{m_{pass}} \times 100 \tag{3}$$

m_{pass} is the passing mass of adsorbate from the fixed bed column during the operation time of the column and can be calculated with the following equation [43]:

$$m_{pass} = QC_0 t_{total} \tag{4}$$

The bed mass transfer zone (MTZ) is a necessary parameter for the design of an adsorption column and determines the part of the bed that does not effectively transfer mass. The smaller the MTZ, the better the system conditions and the higher the removal efficiency and it can be defined as follows [44]:

$$MTZ = \left(1 - \frac{t_b}{t_e}\right) H \tag{5}$$

where H (cm) is the bed height and tb and te (min) are the breakdown and saturation times, respectively. Breakdown and saturation time is equivalent to the time when C/C_0 reaches 0.05 and 0.95, respectively.

2.6. Bed modeling

For the possibility of predicting the concentration-time profile or breakthrough curve at various operating conditions in adsorption columns, which is essential for the successful design of a column adsorption process, several models have been developed and applied. To describe the dynamic behavior of cobalt adsorption process by algae in continuous systems following models were used to examine the fit with the experimental data.

2.6.1. Thomas model

The Thomas model is based on the mass balance equation, assuming that adsorption equilibrium follows the Langmuir isotherm under the condition of negligible axial dispersion. This model can predict the theoretical breakthrough curve using experimental outlet concentration time data, and thereby determine the amount of metal adsorbed per unit mass of adsorbent in the column [45]. The Thomas model was applied in this study, as expressed by Eq. (6).

$$\frac{C}{C_0} = \frac{1}{1 + \exp\left[k_{Th}\left(\frac{q_{Th} M}{Q} - C_0 t\right)\right]} \tag{6}$$

where k_{Th} and q_{Th} are parameters of the Thomas model, respectively, indicating the adsorption rate constant (L/mg.min) and the maximum adsorption capacity (mg/g), and M is the mass of the adsorbent in the column (g), Q is the flow rate (mL/min), C_0 is the initial concentration (mg/L) and C is the concentration (mg/L) at any time t (min).

2.6.2. Yoon-Nelson model

The Yoon-Nelson model is based on the assumption that the rate of reduction of the adsorption probability for each adsorbed molecule is directly proportional to the adsorption probability and the repulsion probability [46]. The Yoon-Nelson model was applied in this study, as expressed by Eq. (7).

$$\frac{C}{C_0}=\frac{1}{1+\exp\left[k_{YN}\left(\tau-t\right)\right]} \tag{7}$$

where k_{YN} is the rate constant (L/min), τ is the time required for 50% adsorption breakthrough (min), and t is the breakthrough time (min).

2.6.3. Adams–Bohart model

The Adams–Bohart model, which is closely related to the bed depth service time (BDST) approach, is based on the surface reaction rate theory and assumes that external and intraparticle mass transfer resistances can be neglected. The Adams–Bohart model effectively describes the initial part of the breakthrough curve [47]. According to the model, the adsorption behavior in a fixed-bed column can be related to the bed depth, Z, and service time, t. The Adams–Bohart model was applied in this study, as expressed by Eq. (8).

$$\frac{C}{C_0}=\frac{1}{1+\exp\left[k_{AB}\left(\frac{N_0 Z}{U}-C_0 t\right)\right]} \tag{8}$$

where Z (cm) is the height of the bed, t (min) is the service time at the breakthrough point, N_0 (mg/L) is the model parameter indicating the adsorption capacity of the adsorbent per unit volume of the bed, K_{AB} (L/mg.min) is the rate constant, C_0 (mg/L) is the inlet adsorbate concentration, C (mg/L) is the adsorbate concentration at time t, U (m/min) is the linear flow velocity. The critical bed height (bed height where $t = 0$) is determined as Eq. (9) [39].

$$Z_0=\frac{U}{k_{AB}N_0}\ln\left(\frac{C_0}{C}-1\right) \tag{9}$$

2.6.4. Belter model

The Belter model is an empirical two-parameter model used to describe the breakthrough curve of a fixed-bed biosorption column. The model can be expressed as [39]:

$$\frac{C}{C_0}=\frac{1}{2}\left[1+\mathrm{e}rf\left(\frac{t-t_{0.5}}{\sigma\sqrt{2}}\right)\right] \tag{10}$$

where erf(x) is the error function, $t_{0.5}$ is the time at which C/C_0=0.5, and σ is the standard deviation of the linear portion of the breakthrough curve.

3. Results and discussion

3.1. Biosorption characterization

FTIR spectra were taken to characterize the characteristic functional groups present in algae that could be responsible for the biosorption of Cobalt ions. Fig. 1 presents the information of FTIR spectra of *Sargassum sp.* within the spectral range from 500 to 4000 cm^{-1} before and after adsorption. The main peak 3385 cm^{-1} in the wavenumber region between 3000 and 3600 cm^{-1} before adsorption is attributed to O-H stretching from hydroxyl group and amine and amide groups of amino acids. The peak at the wave number 2924 cm^{-1} is attributed to the C–H stretching vibrations of methylene groups (CH_2) and weak peak created in 2358 cm^{-1} related to the stretching vibrations of –NH, $–NH^+$ and $–NH^{2+}$ groups. The amide functional group shows C=O stretching (amide I) at 1656 cm^{-1} and a combination of N-H and C-H stretching vibrations (amide II) at 1535 cm^{-1}. The carbohydrate -O-C stretching is characterized by vibrations at 1081 cm^{-1}, and C-O-C bending by vibrations at 1048 cm^{-1}. The main peak at 1426 cm^{-1} corresponds to the bending of methyl groups in the microalgae. Vibrations at 1243 cm^{-1} indicate bending of the carboxylic acid group in the algae. These peaks are related to carboxylate salts (COO–M) where M can be one of alkali and alkaline earth metals, which are naturally present in algae, or sited on with treatment [48-50].

Comparing the IFTR spectrum before and after the adsorption process shown in Fig. 1, it can be seen that the band corresponding to the hydroxyl, amine, amide, methylene, carboxyl functional groups has shifted. This change in the position of the peaks shows that these functional groups have the largest contribution in the cobalt metal adsorption mechanism.

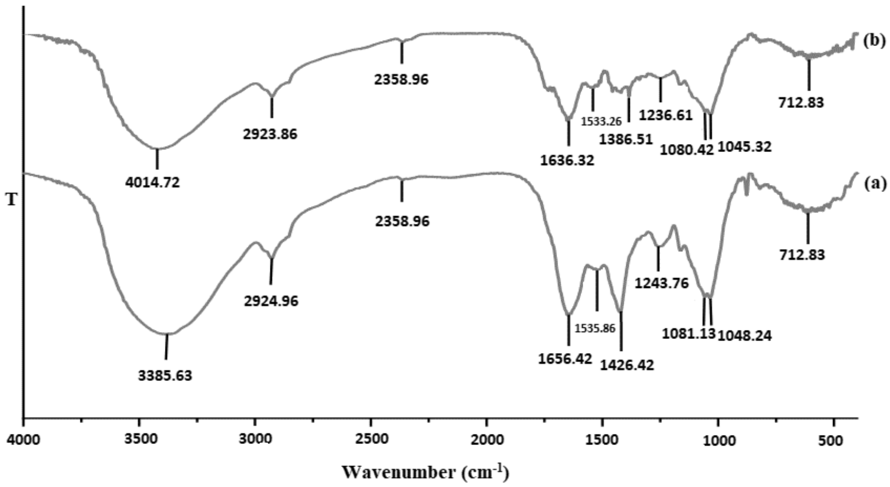

Fig. 1. FTIR spectra of the of *Sargassum sp.* (a) before and (b) after biosorption

Fig. 2 shows the morphology of the *Sargassum sp.* biomass before (a) and after (b) modified with $MgCl_2$ as well as before (b) and after (c) cobalt adsorption. As it is evident from the figure, clear changes in the surface structure have occurred after pretreatment and then adsorption process. Numerous small grooves present on the biomass surface diminished following adsorption (Fig. 2c); which demonstrates the effective uptake of cobalt by the biomass. Other researchers have also reached similar conclusions [49, 51].

3.2. Effect of operating parameters

Adsorption of heavy metal ions by biological cells in continuous systems is influenced by several parameters. These parameters include specific microorganism surface properties and solution physico-chemical properties such as pH, temperature, metal ion concentration in solution, bed height, and inlet flow rate. The effects of some of these parameters, such as pH and temperature, have been investigated and determined in discontinuous experiments, although their effects can be studied again in a continuous system. In the continuous system, the shape and sharpness of the breakthrough curve especially depends on several parameters such as the inlet solution flow rate, the initial adsorbate concentration in solution and the height of the bed, which can be obtained at specified values of pH and temperature. The adsorption capacity of a fixed bed column with certain dimensions depends on the sorption rate, the equilibrium relationship between the adsorbate and the adsorbent, and the mass transfer mechanism. In the following, the effect of the parameters of inlet solution flow rate, initial concentration of adsorbate and bed height has been investigated.

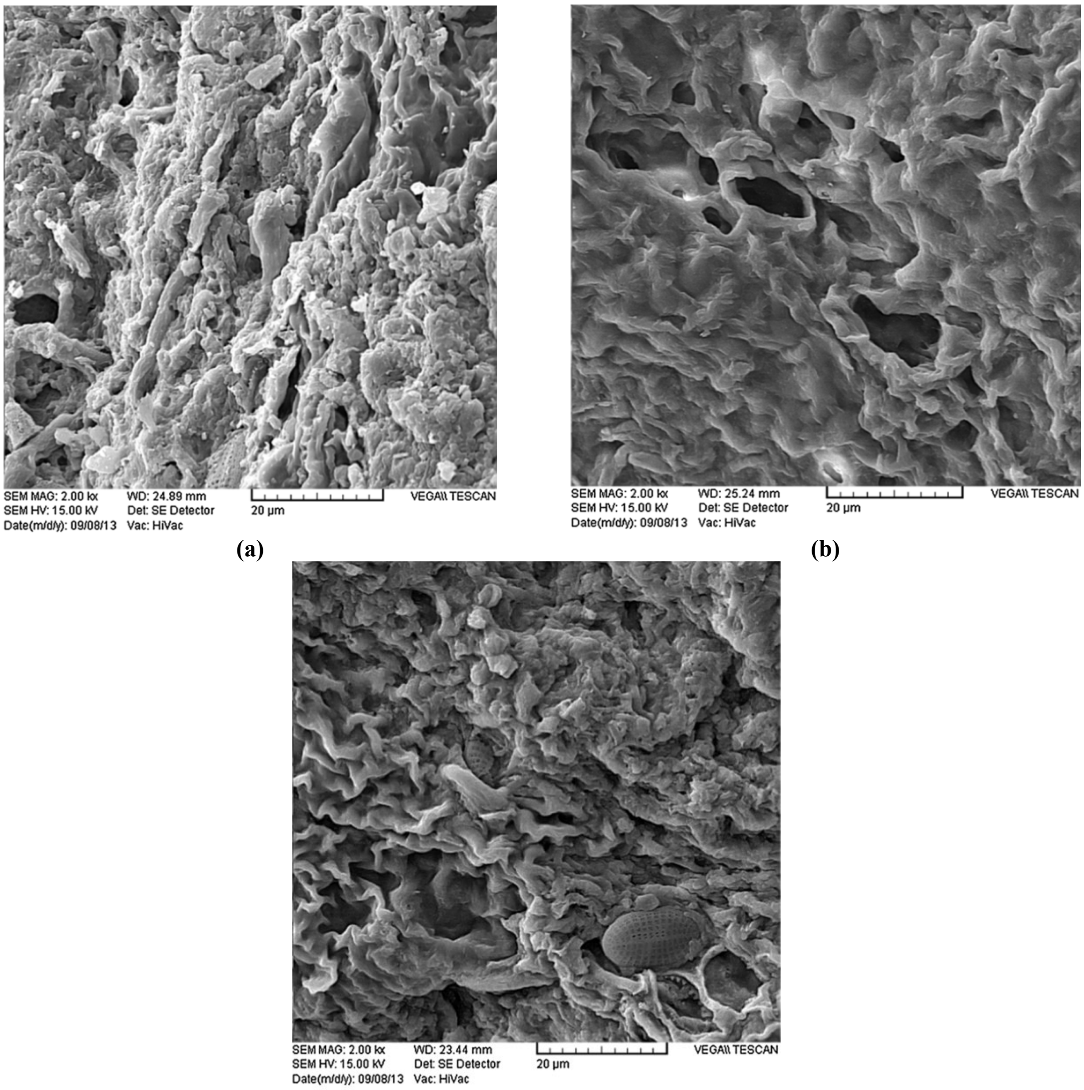

(c)

Fig. 2. SEM images of surface structure of *Sargassum sp.* biomass before (a) and after (b) modification, and after cobalt adsorption (c)

3.2.1. Effect of inlet solution flow rate

One of the main effective parameters in the performance of the adsorption column is the inlet flow rate of the under-treatment solution. In order to investigate the effect of the flow rate of the inlet solution on the adsorption of cobalt ions by the *Sargassum sp.* biomass, the solution adjusted to pH of 7 at a temperature of 25 °C in the flow rate range of 1-4 mL/min was passed through a column with a bed height of 4 cm. Fig. 3 illustrates the breakthrough curves recorded at different flow rates, and Table 1 summarizes the column parameters.

According to the laboratory results presented in Table 1, with an increase in flow rate from 1 to 4 mL/min, the breakthrough time decreases from 50 to 19 minutes, and a decrease in the exhaustion time from 437 to 292 is seen. Furthermore, at the exhaustion point, increasing the flow rate from 1 to 4 mL/min led to a decline in the column's adsorption capacity, from 46.39 to 33.44 mg/g, indicating that higher flow rates reduce contact time and, consequently, the metal uptake. This behavior may be attributed to a more limited interaction time between the solution and the adsorbent at higher flow rates, which can lead to a less favorable mass-transfer condition and reduced column performance. Although the total volume of treated solution increases significantly. Considering that the cobalt adsorption capacity at the flow rate of 1 mL/min was higher than other flow rates (Table 1) and the high removal efficiency, the best performance was obtained at the lowest flow rate.

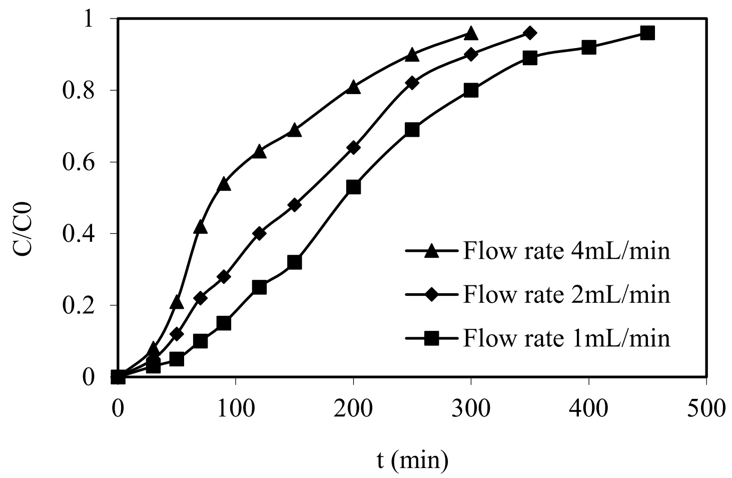

Fig. 3. Effect of flow rate on breakthrough curve for Co adsorption on *Sargassum sp.* algae (bed height 4 cm, feed concentration 50 mg/g)

Table 1. Breakthrough curve parameters for the fixed-bed column for Co ions biosorption by *Sargassum sp.*

Flow rate (mL/min)	Bed height (cm)	C_0 (mg/L)	t_b (min)	q_b (mg/g)	t_e (min)	q_e (mg/g)
1	4	50	50	8.26	437	46.39
1	4	90	34	9.84	340	57.31
1	4	150	22	11.89	300	68.36
1	6	50	61	9.77	440	56.89
1	9	50	70	10.29	450	67.27
1	9	150	64	12.34	428	79.83
2	4	50	30	6.23	342	40.12
4	4	50	19	4.35	292	33.44

This is due to the fact that the longer residence time at reduced flow rates enhances the effectiveness of intra-particle diffusion within the column. Therefore, adsorbate cobalt ions have enough time to diffuse into the deep pores, which increases the removal efficiency and improves the adsorption capacity.

3.2.2. Effect of initial concentration of adsorbate

In order to investigate the effect of the initial concentration of adsorbate of the inlet solution on the adsorption of cobalt ions by the *Sargassum sp.* biomass, the solution adjusted to pH of 7 at a temperature of 25 °C for initial concentration range of 50-150 mg/L was passed through a column with a bed height of 4 cm with flow rate of 1 mL/min. The breakthrough curves obtained at various flow rates are shown in Fig. 4 and the parameters of the column are given in Table 1. According to the laboratory results presented in Table 1, by increasing the inlet concentration from 50 to 150 mg/L, the breakthrough time decreases from 50 to 22 minutes, and a decrease in the exhaustion time from 437 to 300 is seen. Moreover, at the exhaustion point, increasing the initial cobalt concentration from 50 to 150 mg/L resulted in an increase in the column adsorption capacity from 46.39 to 68.36 mg/g, indicating that higher influent concentrations enhance the driving force for mass transfer and, consequently, the metal uptake.

Although the total cobalt removal percentage obtained at lower inlet concentrations are higher than those of higher inlet concentrations of cobalt, it is seen the maximum specific cobalt uptake increased with an increase of inlet cobalt concentration from 50-150 mg/L owing to the large difference in concentration between the sorbate surface and the metal ion solution.

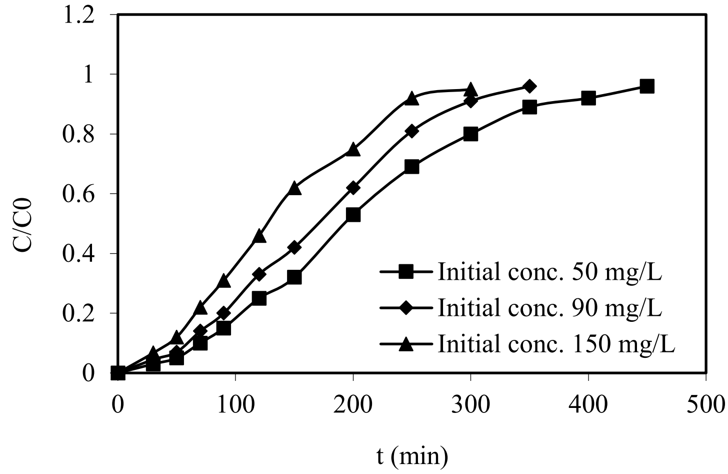

Fig. 4. Effect of inlet concentration on cobalt biosorption by *Sargassum sp.* (bed height 4 cm, feed flow rate: 1 mL/min)

3.2.3. Effect of bed height

The breakthrough curves corresponding to different bed heights are illustrated in Fig. 5, and the operational parameters of the adsorption column are summarized in Table 1. As observed, the breakthrough time noticeably increases with the rise in bed height, which can be attributed to the higher amount of available active sites, longer contact time between the adsorbate and adsorbent.

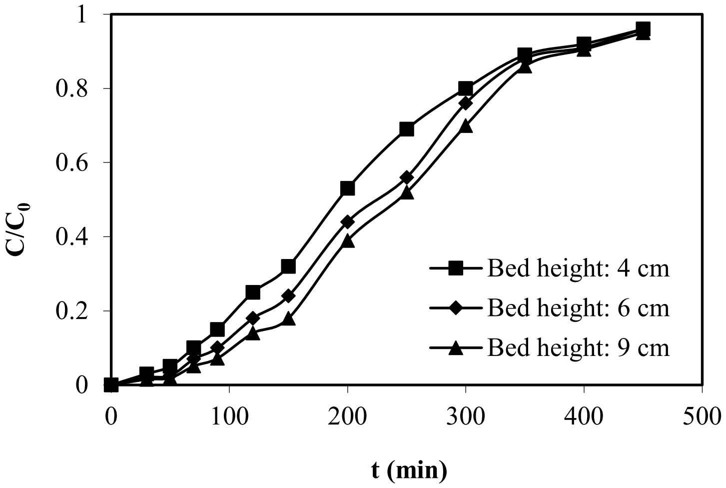

Fig. 5. Effect of contact time on cobalt biosorption by *Sargassum sp.* (inlet concentration 50 mg/L, feed flow rate: 1 mL/min)

According to the laboratory results presented in Table 1, by increasing the bed height from 4 to 9 cm, the breakthrough time increases from 50 to 70 minutes, and an increase in the exhaustion time from 437 to 450 is seen. At the exhaustion point, increasing the bed height from 4 to 9 cm resulted in an increase in the column adsorption capacity from 46.39

to 67.27 mg/g, indicating that a taller bed provides more adsorbent surface area and contact time, thereby enhancing the metal uptake. Additionally, increasing the bed height led to the development of a wider mass transfer zone, resulting in moderately steep breakthrough curves. Furthermore, the total uptake of Co ions increased as the bed height increased, reflecting enhanced adsorption efficiency within the column.

3.3. Modeling of breakthrough curves

The model parameters along with the correlation coefficients (R^2) values for the Thomas, Yoon–Nelson, Adams–Bohart, and Belter models are summarized in Table 2. Although the Yoon–Nelson and Belter models showed slightly lower Root Mean Square Error (RMSE) values, the differences were statistically insignificant. The Thomas model was selected as the most appropriate model because it provided physically meaningful parameters, particularly the equilibrium adsorption capacity (q_{Th}) and Thomas rate constant (k_{Th}), which are essential for evaluating adsorbent performance and designing fixed-bed adsorption systems. Therefore, considering both statistical accuracy and model interpretability, the Thomas model was considered the best model for describing Co (II) breakthrough behavior. As observed in this table, the predicted q_{Th} values obtained from the Thomas model are in good agreement with the corresponding experimental q_e values.

The maximum Co (II) adsorption capacity obtained in the present fixed-bed column study (81.93 mg/g based on Thomas model) was compared with previously reported biosorption studies (Table 3).

Table 2. Isotherm constants for Co biosorption by *Sargassum sp.*

Model	Parameters	Value
Thomas	k_{Th} (L/min.mg)	1.15×10^{-5}
	q_{Th} (mg/g)	81.93
	R^2	0.9901
	RMSE	0.0332
Adams–Bohart	K_{AB} (L/min.mg)	1.92×10^{-4}
	N_0 (mg/L)	2470
	R^2	0.9825
	RMSE	0.0448
Yoon–Nelson	K_{YN} (1/min)	0.0187
	τ (min)	126.4
	R^2	0.9913
	RMSE	0.0311
Belter	σ	47.1
	$t_{0.5}$ (min)	133.2
	R^2	0.9913
	RMSE	0.0312

Table 3. A comparison of various adsorbents in terms of their ability to adsorb cobalt in a continuous system

Adsorbent	q_{max}	Ref.
Greenhouse crop residue	9.5	[52]
Grafting polymer adsorbent (PP-g-(AN-co-AAc-H_2PO_3))	38.91	[53]
Sugarcane bagasse (SBox)	12.98	[54]
Sargassum wightii	49.97	[51]
Marine green alga *Ulva reticulata*	55.6	[35]
Tectona grandis leaves (biochar)	26.73	[55]
Mg-pretreated *Sargassum sp.*	81.93	Present work

The present study demonstrates the promising performance of Mg-pretreated *Sargassum sp.* for cobalt removal in a fixed-bed column, some limitations should be considered. These include the need for regeneration and reuse studies, the possible effect of competitive ions in real wastewater, variability in the composition of marine biomass, and proper management of the cobalt-loaded spent adsorbent. Therefore, further investigations are required to evaluate the long-term practical applicability of this biosorbent under real operating conditions.

4. Conclusion

The *Sargassum sp*. brown algae pretreated with $Mg(NO_3)_2$ exhibited excellent performance for cobalt biosorption in fixed-bed column experiments. The optimal operating conditions were determined as a flow rate of 1 mL/min, a bed height of 9 cm, and an initial cobalt concentration of 150 mg/L, under which the adsorption reached 79.83 mg/g. Characterization by FTIR spectroscopy and SEM imaging before and after biosorption confirmed that *Sargassum sp.* biomass is an effective biosorbent for cobalt removal. Breakthrough curve predictions were carried out using the Thomas, Adams–Bohart, Belter, and Yoon–Nelson models. Although all four models provided reasonably good descriptions of the experimental breakthrough data, considering both statistical accuracy and model interpretability, the Thomas model was considered the best model for describing Co(II) breakthrough behavior.

Nomenclature

Symbols

C	Effluent (outlet) concentration at time t (mg/L)
C_0	Initial (inlet) concentration (mg/L)
H	Bed height (cm)
k_{AB}	Adams–Bohart rate constant (L/mg·min)
K_{Th}	Thomas rate constant (L/mg·min)
k_{YN}	Yoon–Nelson rate constant (L/min)
M	Dry mass of adsorbent in the column (g)
m_{ad}	Mass of adsorbate adsorbed onto solid phase (mg)
m_{pass}	Total mass of adsorbate passed through the column (mg)
N_0	Adams–Bohart adsorption capacity per unit bed volume (mg/L)
Q	Inlet flow rate (mL/min)
q	Adsorption capacity (mg/g)
q_b	Adsorption capacity at breakthrough point (mg/g)
q_e	Equilibrium (exhaustion) adsorption capacity (mg/g)
q_{Th}	Thomas maximum adsorption capacity (mg/g)
$R\%$	Removal efficiency (%)
t	Time (min)
t_b	Breakthrough time ($C/C_0 = 0.05$) (min)
t_e	Exhaustion/saturation time ($C/C_0 = 0.95$) (min)
t_{total}	Total column operation time (min)
$t_{0.5}$	Time at which $C/C_0 = 0.5$ (Belter model) (min)
U	Linear flow velocity (m/min)
Z	Bed height (used in Adams–Bohart model) (cm)
Z_0	Critical bed height (where t=0) (cm)
σ	Standard deviation in Belter model
τ	Time for 50% breakthrough (Yoon–Nelson) (min)

Abbreviation

BDST	Bed Depth Service Time
FTIR	Fourier Transform Infrared Spectroscopy
ICP-AES	Inductively Coupled Plasma Atomic Emission Spectroscopy
MTZ	Mass Transfer Zone
RMSE	Root Mean Square Error
SEM	Scanning Electron Microscopy

References

[1] Munzeiwa, W.A., Ruziwa, D.T., Chaukura, N., 2022. Environmental pollutants: Metal(loid)s and radionuclides. In: Biotechnology for Environmental Protection, Springer, 1–23. https://doi.org/10.1007/978-981-19-4937-1_1

[2] Afolabi, S.S., Zakariyah, M.O., Abedi, M.H., Shafik, W., 2021. A survey on cobalt metallurgical processes and its application, Journal of the Indian Chemical Society, 98 (11), 100179. https://doi.org/10.1016/j.jics.2021.100179

[3] Paustenbach, D.J., Tvermoes, B.E., Unice, K.M., Finley, B.L., Kerger, B.D., 2013. A review of the health hazards posed by cobalt, Critical Reviews in Toxicology, 43 (4), 316–362. https://doi.org/10.3109/10408444.2013.779633

[4] Linna, A., 2023. Effects of Cobalt Exposure on the Respiratory System and the Heart Among Cobalt Production Workers. Tampere University. https://trepo.tuni.fi/bitstream/handle/10024/145306/978-952-03-2747-7.pdf?sequence=2

[5] Thyssen, J.P., 2011. Nickel and cobalt allergy before and after nickel regulation–evaluation of a public health intervention, Contact Dermatitis, 65, 1–68. https://doi.org/10.1111/j.1600-0536.2011.01957.x

[6] Askari Rezaloo, M., Darestani Farahani, N., Bakhshzad Mahmoudi, M., 2024. Simulation investigation of fluorine cold plasma interaction with cobalt oxide as an etchant for decontamination metal waste, Journal of Nuclear Research and Applications, 4 (1), 1–10. https://doi.org/10.24200/jon.2024.1000

[7] Djoudi, N., Le Page Mostefa, M., Muhr, H., 2019. Precipitation of cobalt salts for recovery in leachates, Chemical Engineering & Technology, 42 (7), 1492–1499. https://doi.org/10.1002/ceat.201800696

[8] Servi, I., Turnbull, D., 1966. Thermodynamics and kinetics of precipitation in the copper-cobalt system, Acta Metallurgica, 14 (2), 161–169. https://doi.org/10.1016/0001-6160(66)90297-5

[9] Li, Y., Yang, L., Xu, Z., Sun, Q., 2017. Separation and recovery of heavy metals from waste water using synergistic solvent extraction, IOP Conference Series: Materials Science and Engineering, 167 (1), 012005. https://doi.org/10.1088/1757-899X/167/1/012005

[10] Swain, B., Cho, S.-S., Lee, G.H., Lee, C.G., Uhm, S., 2015. Extraction/separation of cobalt by solvent extraction: A review, Applied Chemistry for Engineering, 26 (6), 631–639. https://doi.org/10.14478/ace.2015.1120

[11] Dehghan, I., Khamseh, A.A.G., Ghadiri, A., 2024. Solvent extraction of uranium from leach liquor using dibutyl carbitol: Optimization of parameters by response surface methodology, Journal of Radioanalytical and Nuclear Chemistry, 333 (3), 1243–1252. https://doi.org/10.1007/s10967-024-09356-2

[12] Khani, M., Khamseh, A.G., 2026. Removal of Sr(II) from aqueous solutions by adsorption using Amberlite XAD-7 resin impregnated with TOPO extractant, Scientific Reports, 16, 8067. https://doi.org/10.1038/s41598-026-39402-w

[13] Bashir, A., Malik, L.A., Ahad, S., Manzoor, T., Bhat, M.A., Dar, G., et al., 2019. Removal of heavy metal ions from aqueous system by ion-exchange and biosorption methods, Environmental Chemistry Letters, 17 (2), 729–754. https://doi.org/10.1007/s10311-018-00828-y

[14] Rodríguez, A., Sáez, P., Díez, E., Gómez, J.M., García, J., Bernabé, I., 2019. Highly efficient low-cost zeolite for cobalt removal from aqueous solutions: Characterization and performance, Environmental Progress & Sustainable Energy, 38 (S1), S352–S365. https://doi.org/10.1002/ep.13057

[15] Mousavi, S.E., Kalal, H.S., Ghorbanian, S.A., Khamseh, A.A.G., Khanchi, A.R., 2023. A comparison of various XAD-Amberlite resins impregnated with dicyclohexyl-18-crown-6 for strontium removal, Progress in Nuclear Energy, 166, 104965. https://doi.org/10.1016/j.pnucene.2023.104965

[16] Jia, F., Yin, Y., Wang, J., 2018. Removal of cobalt ions from simulated radioactive wastewater by vacuum membrane distillation, Progress in Nuclear Energy, 103, 20–27. https://doi.org/10.1016/j.pnucene.2017.11.008

[17] Nour, A., Iqbal, W., Navarro-Alapont, J., Ferrando-Soria, J., Magarò, P., Elliani, R., et al., 2024. Efficient nickel and cobalt recovery by metal–organic framework-based mixed matrix membranes (MMM-MOFs), ACS Sustainable Chemistry & Engineering, 12 (32), 12014–12028. https://doi.org/10.1021/acssuschemeng.4c03427

[18] Aloufi, A.S., Al Riyami, B., Fawzy, M.A., Al-Yasi, H.M., Koutb, M., Hassan, S.H., 2024. Model-assisted optimization of cobalt biosorption on macroalgae Padina pavonica for wastewater treatment, Water, 16 (6), 887. https://doi.org/10.3390/w16060887

[19] Elsherif, K.M., Ewlad-ahmed, A.M., Eldali, A., Saad, R.A., Treban, A.A., 2025. A comprehensive study on adsorption kinetics and equilibrium: Utilizing olive mill by-products as a sustainable biosorbent for cobalt(II) removal, Environmental Research and Technology, 8 (2), 315–327. https://doi.org/10.35208/ert.1510237

[20] Amin, S., Alavi, S., Yousefnia, H., Aghayan, H., 2023. RSM-based investigation of cesium removal from aqueous media with nanocomposites prepared by spherical mesoporous silica and potassium metal hexacyanoferrate, Journal of Nuclear Research and Applications, 3 (2), 32–48. https://doi.org/10.24200/nst.2023.0624

[21] Moghtaderi, S., Saberyan, K., Sid Kalal, H., Mozaffari, S., Khamseh, A.A.G., Nozad Golikand, A., 2024. Investigation of the iridium adsorption process with functionalized magnetic nanoparticles using triisobutylphosphine sulfide extractors, Scientific Reports, 14 (1), 25756. https://doi.org/10.1038/s41598-024-77551-y

[22] Khamseh, A.G., Khani, M., 2025. Enhancing the adsorption of strontium(II) using TOPO impregnated Dowex 50 W-X8 resin, Scientific Reports, 15 (1), 16873. https://doi.org/10.1038/s41598-025-01661-4

[23] Rashid, R., Shafiq, I., Akhter, P., Iqbal, M.J., Hussain, M., 2021. A state-of-the-art review on wastewater treatment techniques: The effectiveness of adsorption method, Environmental Science and Pollution Research, 28 (8), 9050–9066. https://doi.org/10.1007/s11356-021-12395-x

[24] Abbas, S.H., Ismail, I.M., Mostafa, T.M., Sulaymon, A.H., 2014. Biosorption of heavy metals: A review, Journal of Chemical Science and Technology, 3 (4), 74–102. https://www.researchgate.net/publication/266795209_Biosorption_of_Heavy_Metals_A_Review

[25] Kanamarlapudi, S., Chintalpudi, V.K., Muddada, S., 2018. Application of biosorption for removal of heavy metals from wastewater, Biosorption, pp. 70–116. https://doi.org/10.5772/intechopen.77315

[26] Abdi, O., Kazemi, M., 2015. A review study of biosorption of heavy metals and comparison between different biosorbents, Journal of Materials and Environmental Science, 6 (5), 1386–1399. https://www.researchgate.net/publication/281951859

[27] Khani, M., Khamseh, A.G., 2023. Statistical analysis, equilibrium and dynamic study on the biosorption of strontium ions on Chlorella vulgaris, Journal of Radioanalytical and Nuclear Chemistry, 332 (8), 3325–3334. https://doi.org/10.1007/s10967-023-09026-9

[28] Romera, E., González, F., Ballester, A., Blázquez, M., Muñoz, J., 2007. Comparative study of biosorption of heavy metals using different types of algae, Bioresource Technology, 98 (17), 3344–3353. https://doi.org/10.1016/j.biortech.2006.09.026

[29] Bulgariu, D., Bulgariu, L., 2012. Equilibrium and kinetics studies of heavy metal ions biosorption on green algae waste biomass, Bioresource Technology, 103 (1), 489–493. https://doi.org/10.1016/j.biortech.2011.10.016

[30] Soleymani, F., Khani, M., Pahlevanzadeh, H., Amini, Y., 2023. Intensification of strontium(II) ion biosorption on Sargassum sp. via response surface methodology, Scientific Reports, 13 (1), 5403. https://doi.org/10.1038/s41598-023-32532-5

[31] Khani, M., Keshtkar, A., Ghannadi, M., Pahlavanzadeh, H., 2008. Equilibrium, kinetic and thermodynamic study of the biosorption of uranium onto Cystoseria indica algae, Journal of Hazardous Materials, 150 (3), 612–618. https://doi.org/10.1016/j.jhazmat.2007.05.010

[32] Khani, M., 2013. Biosorption of strontium by Padina sp. algae biomass: Process optimisation and equilibrium study, International Journal of Environmental Technology and Management, 16 (4), 290–311. https://doi.org/10.1504/IJETM.2013.054823
[33] Liu, C., Wen, X., Pan, H., Luo, Y., Zhou, J., Wu, Y., et al., 2024. Bioremoval of Co(II) by a novel halotolerant microalgae Dunaliella sp. FACHB-558 from saltwater, Frontiers in Microbiology, 15, 1256814. https://doi.org/10.3389/fmicb.2024.1256814
[34] Soleymani, F., Khani, M., Pahlavanzadeh, H., Manteghian, M., 2015. Study of cobalt(II) biosorption on Sargassum sp. by experimental design methodology, International Journal of Environmental Science and Technology, 12 (6), 1907–1922. https://doi.org/10.1007/s13762-014-0739-0
[35] Vijayaraghavan, K., Jegan, J., Palanivelu, K., Velan, M., 2005. Biosorption of copper, cobalt and nickel by marine green alga Ulva reticulata in a packed column, Chemosphere, 60 (3), 419–426. https://doi.org/10.1016/j.chemosphere.2004.12.016
[36] Albayari, M., Nordin, N., Adnan, R., Khalili, F., Nazal, M., 2024. Biosorption of uranium(VI) and thorium(IV) from aqueous solution by marine Sargassum aquifolium macroalgae, Biomass Conversion and Biorefinery, 14 (19), 23501–23514. https://doi.org/10.1007/s13399-023-04492-3
[37] Wang, X., Shan, T., Pang, S., 2021. Removal of Sr, Co, and Mn from seawater by Sargassum horneri in mono- and multi-nuclide contamination scenarios, Journal of Applied Phycology, 33 (4), 2587–2596. https://doi.org/10.1007/s10811-021-02477-1
[38] Yang, J., Volesky, B., 1999. Biosorption of uranium on Sargassum biomass, Water Research, 33 (15), 3357–3363. https://doi.org/10.1016/S0043-1354(99)00043-3
[39] Riazi, M., Keshtkar, A.R., Moosavian, M.A., 2016. Biosorption of Th(IV) in a fixed-bed column by Ca-pretreated Cystoseira indica, Journal of Environmental Chemical Engineering, 4 (2), 1890–1898. https://doi.org/10.1016/j.jece.2016.03.017
[40] Barquilha, C.E., Cossich, E.S., Tavares, C.R., da Silva, E.A., 2019. Biosorption of nickel and copper ions from synthetic solution and electroplating effluent using fixed-bed column of immobilized brown algae, Journal of Water Process Engineering, 32, 100904. https://doi.org/10.1016/j.jwpe.2019.100904
[41] Amiri, M., Keshtkar, A.R., Moosavian, M.A., 2022. Th(IV) biosorption from a three-component feed solution by Ca-pretreated Cystoseira indica alga in a fixed-bed column: Experimental tests and modeling, Journal of Environmental Chemical Engineering, 10 (6), 108579. https://doi.org/10.1016/j.jece.2022.108579
[42] Riazi, M., Keshtkar, A.R., Moosavian, M.A., 2014. Batch and continuous fixed-bed column biosorption of thorium(IV) from aqueous solutions: Equilibrium and dynamic modeling, Journal of Radioanalytical and Nuclear Chemistry, 301 (2), 493–503. https://doi.org/10.1007/s10967-014-3129-7
[43] Sohbatzadeh, H., Keshtkar, A., Safdari, J., 2021. Investigation of U(VI) biosorption dynamic in fixed-bed column: Calculation of mass transfer resistances and identification of rate-controlling step, Journal of Nuclear Science, Engineering and Technology (JONSAT), 42 (1), 82–91. https://doi.org/10.24200/nst.2021.1188
[44] Keshtkar, A.R., Amiri, M., Moosavian, M.A., 2024. Multicomponent biosorption of U(VI), Cu(II), and Ni(II) in the fixed-bed column: Dynamic mathematical modeling, GWO optimization, and biosorption experiments. Research Square. https://doi.org/10.21203/rs.3.rs-4992859/v1
[45] Limsuwan, Y., Lertsarawut, P., Hemvichian, K., Seko, N., Pongprayoon, T., 2024. Cu(II) removal from aqueous solution in trickle tray adsorber using non-woven fabric modified via radiation-assisted functionalization, Scientific Reports, 14 (1), 27076. https://doi.org/10.1038/s41598-024-78450-y
[46] Nithya, K., Sathish, A., Kumar, P.S., 2020. Packed-bed column optimization and modeling studies for removal of chromium ions using chemically modified Lantana camara adsorbent, Journal of Water Process Engineering, 33, 101069. https://doi.org/10.1016/j.jwpe.2019.101069
[47] Prabhu, A.A., Chityala, S., Jayachandran, D., Deshavath, N.N., Veeranki, V.D., 2021. A two-step optimization approach for maximizing biosorption of hexavalent chromium ions (Cr(VI)) using alginate immobilized Sargassum sp. in a packed-bed column, Separation Science and Technology, 56 (1), 90–106. https://doi.org/10.1080/01496395.2019.1708933
[48] Oliveira, R.C., Hammer, P., Guibal, E., Taulemesse, J.-M., Garcia Jr., O., 2014. Characterization of metal–biomass interactions in the lanthanum(III) biosorption on Sargassum sp. using SEM/EDX, FTIR, and XPS: Preliminary studies, Chemical Engineering Journal, 239, 381–391. https://doi.org/10.1016/j.cej.2013.11.042
[49] Sheng, P.X., Ting, Y.-P., Chen, J.P., Hong, L., 2004. Sorption of lead, copper, cadmium, zinc, and nickel by marine algal biomass: Characterization of biosorptive capacity and investigation of mechanisms, Journal of Colloid and Interface Science, 275 (1), 131–141. https://doi.org/10.1016/j.jcis.2004.01.036
[50] Chen, J.P., Hong, L., Wu, S., Wang, L., 2002. Elucidation of interactions between metal ions and Ca alginate-based ion-exchange resin by spectroscopic analysis and modeling simulation, Langmuir, 18 (24), 9413–9421. https://doi.org/10.1021/la026060v
[51] Vijayaraghavan, K., Jegan, J., Palanivelu, K., Velan, M., 2005. Biosorption of cobalt(II) and nickel(II) by seaweeds: Batch and column studies, Separation and Purification Technology, 44 (1), 53–59. https://doi.org/10.1016/j.seppur.2004.12.003
[52] Blázquez, G., Martín-Lara, M.Á., Iáñez-Rodríguez, I., Morales, I., Pérez, A., Calero, M., 2022. Cobalt biosorption in fixed-bed column using greenhouse crop residue as natural sorbent, Separations, 9 (10), 316. https://doi.org/10.3390/separations9100316
[53] Maleki, F., Gholami, M., Torkaman, R., Torab-Mostaedi, M., Asadollahzadeh, M., 2021. Cobalt(II) removal from aqueous solution by modified polymeric adsorbents prepared with induced-graft polymerization: Batch and continuous column study with analysis of breakthrough behaviors, Environmental Technology & Innovation, 24, 102054. https://doi.org/10.1016/j.eti.2021.102054

[54] Rodrigues, J.A.V., Martins, L.R., Furtado, L.M., Xavier, A.L.P., Almeida, F.T.R., Moreira, A.L.S.L., et al., 2020. Oxidized renewable materials for the removal of cobalt(II) and copper(II) from aqueous solution using batch and fixed-bed column adsorption, Advances in Polymer Technology, 2020 (1), 8620431. https://doi.org/10.1155/2020/8620431

[55] Vilvanathan, S., Shanthakumar, S., 2017. Column adsorption studies on nickel and cobalt removal from aqueous solution using native and biochar form of Tectona grandis, Environmental Progress & Sustainable Energy, 36 (4), 1030–1038. https://doi.org/10.1002/ep.12567